International Journal of Applied Engineering Research ISSN 0973-4562 Volume 11, Number 11 (2016) pp 7541-7549

Impact of Orifice Jet Configuration on Heat Transfer in a Channel with Inclined Target Surface Cooled by Single Array of Impinging Jets with Outflow Opposing the Entry Flow

Ali A. Al-Mubarak*, S. M. Shaahid and Luai M. Al-Hadhrami *****
** Scientist Researcher, **Research Engineer, *** Associate Professor*
Center for Engineering Research, Research Institute
King Fahd University of Petroleum and Minerals
Dhahran 31261, Saudi Arabia.

Abstract
An experimental investigation has been carried out to study the effect of origice-jet plate configuration on heat transfer characteristics in a channel with inclined heated target plate cooled by single array of equally spaced impinging jets. Air ejected from an array of orifices is aimed at the heated target surface and exits from the radial outlets. The target plate forms the leading edge of a gas turbine blade. The study covers the effect of various orifice-jet plate configurations, feed channel aspect ratios ($5 \leq H/d \leq 9$) and Reynolds number ($9300 \leq Re \leq 18800$) on the heat transfer characteristics for a given outflow orientation (outflow direction opposing the entry flow). Three orifice-jet plate configurations (centered, staggered, and tangential holes) have been examined. In general, it has been noticed that Nusselt number (Nu) is high for higher aspect ratios. For a given plate-1 with single array of equally spaced centered jets and for Re=18800 (outflow opposing the entry flow), the local Nu for H/d=9 has been found to be greater than Nu of H/d=7 by 5%. This increase can be attributed to increase in strength of impinging jets due to increase in feed channel aspect ratio. It has also been noticed that plate-1 with centered orifice-jet configuration gives better heat transfer characteristics relatively as compared to other orifice-jet configurations. The percentage increase in average Nu has been found to be about 19% with centered holes as compared staggered orifice-jet plate. The percentage increase in average Nu has been found to be about 4% with staggered jet-plate as compared to tangential orifice-jet plate configuration.

INTRODUCTION

Jet impingement heat transfer has become well established as a high-performance technique for convectively heating, cooling (example in gas turbines), or drying a surface. Gas turbines are used for aircraft propulsion and for land-based power generation. The efficiency of advanced gas turbines can be improved by increasing the inlet gas temperature. To accommodate higher inlet temperatures in gas turbines and still maintain the metal temperatures below acceptable limits, highly sophisticated cooling techniques are required. Development in turbine cooling technology plays an important role in increasing the thermal efficiency and power output of gas turbines. Impingement heat transfer is considered as a promising heat transfer enhancement technique. Impinging jets are widely used where high rates of heat transfer are desired. Among all convection heat transfer enhancement methods, it provides significantly high local heat transfer coefficient. At the surface where a large amount of heat is to be removed or added, this technique can be employed directly through very simple design involving a plenum chamber and orifices. For instance, in gas turbine cooling, jet impingement heat transfer is suitable for cooling the leading edge of a rotor airfoil. This technique is also employed in turbine guide vanes (stators). In modern gas turbine design, the trend is toward high inlet gas temperature (1600 – 1800 ^{o}K) for improving thermal efficiency and power density. Since these temperatures are far above the allowable metal temperature, the gas turbine blades must be cooled in order to operate without failure. Broad range of parameters affect the heat transfer distribution, like impinging jet Re, jet size, target surface geometry, spacing of the target surface from the jet orifices, orifice-jet plate configuration, outflow orientation, etc. Literature indicates that many of these parameters have been studied experimentally and theoritically in appreciable depth [1-20].

Chupp et al. [1] studied the heat transfer characteristics for the jet impingement cooling of the leading edge region of a gas turbine blade. Flourscheutz et al. [2] investigated the heat transfer characteristics of jet array impingement with the effect of initial crossflow. Metzger and Bunker [3] and Flourscheutz et al [4] used the liquid crystal technique to study the local heat transfer coefficients. The authors observed that the jet Nusselt number depends mainly on the jet Reynolds number.

Dong et al [5] determined experimentally the heat transfer characteristics of a premixed butane/air flame jet impinging upwards on an inclined flat plate at different angles of inclination and fixed Reynolds number (Re = 2500) and a plate to nozzle distance of 5d. It was found that the location of maximum heat flux shifted away from impingement point by reducing the angle of incidence. Decreasing the angle of incidence reduced the average heat transfer. Rasipuram and Nasr [6] studied air jet issuing out of defroster's nozzles and impinging on inclined windshield of a vehicle. The overall heat transfer coefficient of the inclined surface for the configuration with one rectangular opening was found to be 16% more than that for the configuration with two rectangular openings. Beitelmal et al [7] investigated the effect of inclination of an impinging air jet on heat transfer characteristics. They found that maximum heat transfer shifts

towards the uphill side of the plate and the maximum Nusselt number (Nu) decreases as the inclination angle decreases. Roy and Patel [8] studied the effect of jet angle impingement on local Nu and nozzle to target plane spacing at different Re. They found that heat transfer is the maximum through the shear layer formed near the jet attachment stagnation region. Ekkad et al [9] studied the effect of impinging jet angle ±45 on target surface by using transient liquid crystal technique for single Re = 1.28×10^4. It has been noted that the orthogonal jets provide higher Nu as compared to angled jets.

Tawfek [10] investigated the effect of jet inclination on the local heat transfer under an obliquely impinging round air jet striking on circular cylinder. Their results indicated that with increase in inclination, the upstream side of heat transfer profile dropped more rapidly than the downstream side. Seyedein et.al. [11] performed numerical simulation of two dimensional flow fields and presented the heat transfer due to laminar heated multiple slot jets discharging normally into a converting confined channel by using finite difference method with different Re (600-1000) and angle of inclination (0-20°). It has been observed that the inclination has a leveling effect on the Nu, distribution over the impingement surface. Yang and Shyu [12] presented numerical predictions of heat transfer characteristics of multiple impinging slot jets with an inclined confinement surface for different angles of inclination and different Re. The results showed that the local Nu downstream increases with increasing inclination of angle. Yan and Saniei [13] dealt with measurement of heat transfer coefficient of an impinging circular air jet to a flat plate for different oblique angles (45-90°) and different Re (10000 & 23000) by using transient liquid crystal technique. The results showed that the point of maximum heat transfer shifts away from the geometrical impingement point toward the compression side of the wall jet on the axis of symmetry.

Hwang et. al [14] studied the heat transfer in leading edge triangular duct by an array of wall jets with different Re (3000-12600) and jet spacing s/d (1.5-6) by using transient liquid crystal technique on both principal walls forming the apex. Results show that an increase in Re increases the Nu on both walls. Ramiraz et al [15] investigated the convective heat transfer of an inclined rectangular plate with blunt edge at various Re (5600-38500) and angle of inclination (60-70°). The heat transfer distribution over a finite rectangular plate was found to be very much dependent on the orientation of the plate. Stevens and Webb [16] examined the effect of jet inclination on local heat transfer under an obliquely impinging round free liquid jet striking at different Re, angle of inclination, and nozzle sizes. It was found that the point of maximum heat transfer along the x-axis gets shifted upstream.

Hwang and Cheng [17] performed an experimental study to measure local heat transfer coefficients in leading edge using transient liquid crystal technique. Three right triangular ducts of the same altitude and different apex angles (30º, 45º & 60º) were tested for various jet Re (3000 ≤Re≤12000) and different jet spacing (s/d=3 and 6). Results show that an increase in Re increases the Nu on all the walls. Hwang and Cheng [18] measured experimentally local heat transfer coefficients on two principal walls of triangular duct with swirl motioned airflow induced by multiple tangential jets from the side entry of the duct by using transient liquid crystal technique. The study indicated that the jet inlet angle affects strongly the averaged bottom-wall heat transfer. Hwang and Chang [19] measured heat transfer coefficients on two walls by using transient liquid crystal technique in triangular duct cooled by multiple tangential jets. The results show that an increase in Re, increases heat transfer of both walls. Hwang and Cheng [20] studied heat transfer characteristics in a triangular duct cooled by an array of side-entry tangential jets. Detailed heat ransfer characteristics were determined (using transient liquid crystal technique) for the two walls forming the apex for different jet Re and jet spacings. Results showed that an increase in Re increased the heat transfer on both walls, also a decrease in heat transfer was observed downstream due to crossflow effect. All of the earlier studies observed an increase in heat transfer with jet impingement.

The above work indicates that no study has been conducted to show the effect of different orifice-jet plate configurations on feed channel aspect ratio with different jet Re, for a given outflow orientation (diameter of jet, d = 0.5 cm) on heat transfer in a channel with inclined heated target surface. The objective of the present study includes investigation of the above effects by conducting the experimental work. Specifically, the work includes the effect of three orifice-jet plate configurations (centered holes, staggered holes, tangential holes) and three feed channel aspect ratios (H/d=5, 7, and 9) on the heat transfer characteristics for a given outflow orientation (outflow direction opposing the entry flow; the air after impingement was constrained to exit in a single direction along the channel formed the target surface and the jet plate) and for a given Reynolds number with inclined heated target surface**.** Knowledge of the effect of orifice-jet-plate configuration is essential for achievement of optimal designs. The thrust behind this work is that the channel of turbine blade internal cooling circuit at the leading edge is inclined.

DESCRIPTION OF THE EXPERIMENT

The schematic of the experimental set-up is depicted in Figure 1. The test rig used to study the heat transfer characteristics has been constructed using Plexi-glass. The test section consists of two channels, impingement (10) and the feed channel (9). Air enters the test section in the feed channel and is directed onto the heated copper plates in the impingement channel to study the heat transfer characteristics. The target plates (11), made of copper, were heated using a constant flux heater. The other side of the heater was insulated to get the heat transferred only in one direction. The mass flow rate of the compressed air (1) entering the test section was passed through a settling chamber (5) and was controlled with the help of valves (2). The pressure drop was measured using the pressure gauges (4). Gas flow meter (7) was used to measure the mass flow rate entering the test rig which was protected by the air filters (6) of 50μ capacity.

The average surface temperature of each copper plate was determined from the readings of two T-type thermocouples (12) installed in the holes drilled at the back surface of the plates to within 1 mm of the surface in depth. The analog

signals generated by these temperature sensors were transmitted to the signal-conditioning unit where they were selectively processed. The resulting analog signals were converted into digital signals by a DAQ (13) card and recorded with an application software developed in LabView.

Figure 2.1 shows the three-dimensional sketch of the test section. It consists of two channels joined by the orifice plate, which has a single array of equally spaced (centered or staggered or tangential) orifice jets shown in Figure 3. The jet orifice plate thickness is twice the jet diameter. There are 13 jets on the orifice plate. The jet-to-jet spacing is 8 times the jet diameter and the orifice jet diameter $d = 0.5cm$. The length of the test section is 106.5 cm. The width of the feed channel (H) was varied from 2.5 to 4.5 cm (i.e. H/d=5, 7, 9, d=0.5 cm). The impingement target surface constitutes a series of 13 copper plates, each with 4.2 × 4.1 cm in size, arranged in accordance with the orifice jets such that the impingement jet hits the geometric center of the corresponding plate (however, first and last copper plates are slightly different in sizes). All the copper plates are separated from each other by 1 mm distance to avoid the lateral heat conduction, thus dividing the target surface into segments. The thickness of the copper plate is 0.5 cm. As shown in Figure 2.2, the length of impingement surface L is 57.3 cm (the target surface is inclined at angle 1.5º, the width of parallel flow side "S2" is 2 cm and the width of the opposite flow side "S1" is 3.5 cm).

Figure 4 shows the schematic of the three different outflow orientations, which are obtained by changing the discharge openings (i.e. different crossflow directions are created by changing the test section open ends). The upper channel is called as the feed channel and the lower channel in which the jets impinge on the target surface is called as the impingement channel. The exit of jets in three different outflow orientations from the impingement channel creates different crossflow effects as shown in Fig. 4. However, in the present study, attention is focussed on Case – 2.

Case-1 (Outflow coincident with the entry flow),

Case-2 (Outflow opposing to the entry flow),

Case-3 (Outflow passes out in both the directions).

Figure 5 shows the details of the construction of the target surface. The copper plate is heated with a constant flux heater held between the wooden block and the copper plate by glue (to reduce contact resistance). The ends were sealed with a rubber material to avoid lateral heat losses. The wooden block was 3 cm thick to minimize the heat lost to the surroundings, so that the heat is transferred completely to copper plates only.

PROCEDURE

Tests were carried out using a given orifice-jet plate (centered or staggered or tangential holes) with jet diameter $d = 0.5cm$ for a given jet Reynolds numbers Re = 18800 (for a given H/d ratio, for outflow direction opposing the entry flow direction) and for a constant heat flux power input. The heated target plate was oriented at a pre-defined angle (1.5º). The mass flow rate was adjusted to the required value for the experiment to be conducted and the air was blown continuously into the test section. Heat was supplied to the copper plates with electric resistive constant flux heaters from backside to provide uniform heat flux. The temperature of the copper plates was measured by two thermocouples mounted in a groove of 2.5 mm on the back of the copper plates. Thus the temperature of a particular plate has been taken as the average of the reading of two thermocouples. The temperature of the copper plates, pressure, temperature of the air at the inlet, and the mass flow rate were continuously monitored. After the temperature of the copper plates reached the steady state condition, all the data was collected with Lab VIEW program. The Nusselt number was then calculated based upon the collected data. The same procedure was repeated for the three different orifice-jet plates described in Figures 3a, 3b & 3c and for different aspect ratios (H/d = 5, 7, 9).

Data Reduction and Uncertainty Analysis

The collected data was subjected to uncertainty analysis. The method for performing the uncertainty analysis for the present experimental investigation has been taken from Taylor B.N. [21]. The theory for the current uncertainty analysis is summarized in the following discussion:

Jet Reynolds Number Calculations

The average velocity used to calculate the jet Reynolds number is calculated using the following equation

$$V_{avg} = \frac{\forall}{13 \times \frac{\pi}{4} d^2} \quad (1)$$

The data reduction equation for the jet Reynolds number is taken as:

$$Re = \frac{\rho V_{avg} d}{\mu} = \frac{\rho d}{\mu} \frac{\forall}{13 \times \frac{\pi}{4} d^2} \quad (2)$$

Uncertainty In Jet Reynolds Number

Taking into consideration only the measured values, which have significant uncertainty, the jet Reynolds number is a function of orifice jet diameter and volume flow rate and is expressed mathematically as follows:

$$Re = f(\forall, d) \quad (3)$$

Density and dynamic viscosity of air is not included in the measured variables since it has negligible error in the computation of the uncertainty in jet Reynolds number**.** The uncertainty in Renolds number has been found to be about ± 2.1%.

NUSSELT NUMBER CALCULATION

The total power input to all the copper plates was computed using the voltage and current, the former being measured across the heater, using the following equation:

$$Q_{total} = \frac{V^2}{R} = VI \quad (4)$$

The heat flux supplied to each copper plate was calculated using:

$$q'' = \frac{Q_{total}}{A_{total}} \quad (5)$$

The heater gives the constant heat flux for each copper plate. The heat supplied to each copper plate from the heater is calculated using the following procedure:

$$Q_{cp,i} = q'' \times A_{cp,i} \quad (6)$$

Where i is the index number for each copper plate. The heat lost by conduction through the wood and to the surrounding by radiation is depicted in Figure 5 and has been estimated using the following equations for each plate.

$$Q_{cond,i} = k_{wood} A_{cp,i} \frac{(T_{s,i} - T_w)}{t} \quad (7)$$

$$Q_{rad,i} = \varepsilon \sigma A_{cp,i} (T_{s,i}^4 - T_{surr}^4) \quad (8)$$

The actual heat supplied to each copper plate has been determined by deducting the losses from the total heat supplied to the heater.

$$Q_{actual,i} = Q_{cp,i} - (Q_{cond,i} + Q_{rad,i}) \quad (9)$$

The local convective heat transfer coefficient for each of the copper plate has been calculated using:

$$h_i = \frac{Q_{actual,i}}{A_{cp,i}(T_{s,i} - T_{in})} \quad (10)$$

The average temperature of the heated target surface $T_{s,i}$ has been taken as the average of the readings of the two thermocouples fixed in each copper plate. To calculate h, T_{in} has been considered instead of the bulk temperature or the reference temperature. For a given case (for a given Re, H/d, and orifice-jet plate) T_{in} is fixed. It is measured at the test section inlet, where the air first enters the feed channel. The non-dimensional heat transfer coefficient on the impingement target surface is represented by Nusselt number as follows:

$$Nu_i = \frac{h_i d}{k_{air}} \quad (11)$$

The hydraulic diameter has been taken as the diameter of the orifice jet. The data reduction equation for the Nusselt number is considered along with the heat losses by conduction and radiation.

$$Nu_i = \frac{d}{k_{air}} \left(\frac{\frac{V^2}{R A_{total}} - \frac{k_w}{t}(T_{s,i} - T_w) - \varepsilon\sigma(T_{s,i}^4 - T_{Surr}^4)}{(T_{s,i} - T_{in})} \right) \quad (12)$$

Uncertainty in Nusselt Number

Temperature of the wood has a very less effect on the uncertainty of heat transfer coefficient due to the large thickness of the wood and also due to the insulation material attached to the wooden block. Temperature of the surroundings and emissivity also has less effect on the uncertainty as the work was carried out in a controlled environment and the temperature of the surroundings was maintained within 21-23 $^\circ C$ through out the experiment. The standard uncertainty in the Nusselt number neglecting the covariance has been calculated using the following equation:

$$\left(U_{c,Nu_i}\right)^2 = \left(\frac{\partial Nu_i}{\partial V} u_V\right)^2 + \left(\frac{\partial Nu_i}{\partial R} u_R\right)^2 + \left(\frac{\partial Nu_i}{\partial T_{s,i}} u_{T_{s,i}}\right)^2 + \left(\frac{\partial Nu_i}{\partial T_{in}} u_{T_{in}}\right)^2 + \left(\frac{\partial Nu_i}{\partial A_{total}} u_{A_{total}}\right)^2 + \left(\frac{\partial Nu_i}{\partial d} u_d\right)^2 \quad (13)$$

Uncertainty propagation for the dependent variable in terms of the measured values has been calculated using the Engineering equation Solver (EES) software. The measured variables x_1, x_2 etc. have a random variability that is referred to as its uncertainty. The uncertainty in Nusselt number in the present study has been found to vary between ± 6% depending upon the jet velocity.

RESULTS AND DISCUSSIONS

Jet impingement heat transfer is dependent on several flow and geometrical parameters. The jet impingement Nusselt number is presented in a functional form as follows:

$$Nu_i = \left(\frac{h_i d}{k_{air}}\right) = f\left[\text{Re}, \left(X/d, H/d\right), \textit{outflow orientation}\right] \quad (14)$$

Where, Re is the flow parameter, jet spacing to the diameter ratio (X/d) is the geometric parameter. The flow exit direction and target surface geometry are also important parameters having a considerable impact on impingement heat transfer.

The X location starts from the supply end of the channel as shown in Figure 2.1. For case-1 shown in Figure 4a, flow enters at X/d = 109.3 and exits at X/d = 0. For case-2 (Figure 4b), flow exits at X/d = 109.3. For case-3 (Figure 4c), flow exits at both ends (X/d = 0 and X/d = 109.3). The flow is fully developed before entering the orifice jets. In the present study attention is focused on case – 2 (outflow direction opposing the entry flow).

Effect of Orifice-jet-plate Configuration on Feed Channel Aspect Ratio

In order to show the effect of orifice-jet-plate configuration on feed channel aspect ratio (for outflow direction opposing the entry flow as shown in Figure 4b, and for a given Re= 18800), tests were conducted for three orifice-jet-plate configurations and for three aspect ratios (H/d). Figures 6-8 show the local Nusselt number distribution for three orifice-jet plate configurations and for three H/d ratios as a function of non-dimensional location X/d on the test or heated target surface. In general, it has been observed that Nu is high for higher aspect ratios (higher H/d means more fluid flow due to higher feed channel width and hence enhanced heat transfer). At higher H/d ratios, the pressure losses are less, therefore the heat transfer rates are higher. In other words, the heat transferred from the target surface decreases with a decrease in feed channel width from H/d = 9 to 5. For all the orifice-jet plate configurations, flow enters the feed channel at X/d=109.3. For given plate-1 (single array of equally spaced centered jets, Figure 6, for Re=18800, outflow opposing the entry flow), the local Nu for H/d=9 has been found to be greater than Nu of H/d=7 by 5%. Furthermore, Nu has been found to be relatively high in the mid-portion of the target surface while low at the ends. In a broad perspective, as the air

impinges on the target surface, crossflow starts developing and grows continuously towards the exit resulting into thicker boundary layer.

The air exits at X/d=109.3 (location of exit point is same as the entry point) for all the plates in this study. In this situation, the boundary layer becomes thicker at the exit and hence Nu is less at X/d=109.3. Although, the jet strength is more at entrance (X/d=109.3), but since flow also exits at X/d=109.3, the cross-flow or boundary layer effect is more dominating (i.e. as the flow progresses towards the exit, the cross-flow builds-up and distorts/distracts the impinging jets at X/d=109.3) and results in lower Nu at exit. Also, since the flow exits at X/d=109.3, the hot air becomes stagnant at the closed/other end (X/d=0) of the target surface resulting in decrease in Nu. Similar types of behavior were noticed for orifice jet plate-2 (staggered holes) and orifice jet plate-3 (tangential holes) as can be seen in Figures 7-8.

Figure 6 shows the effect of H/d on local Nusselt number for Re=18800 for orifice jet plate with centered holes. It can be observed that, H/d=9 gives the maximum heat transfer over the entire length of the target surface as compared to all feed channel aspect ratios studied. H/d=9 gives 2% more heat transfer from the target surface as compared to H/d=5. Whereas H/d=5 gives 3% increase in heat transfer as compared to H/d=7. Figure 7 illustrates the effect of H/d on local Nusselt number for Re=18800 for orifice jet plate with staggered jets. It can be observed that, H/d=9 gives the maximum heat transfer over the entire length of the target surface as compared to all feed channel aspect ratios studied. H/d=9 gives 2% more heat transfer from the target surface as compared to H/d=5 whereas H/d=5 gives 6% increase in heat transfer as compared to H/d=7. Figure 8 demonstrates the effect of H/d on local Nusselt number for Re=18800 for orifice jet plate with tangential holes. It can be observed that, H/d=7 gives the maximum heat transfer over the entire length of the target surface as compared to other feed channel aspect ratios studied. H/d=9 gives 8% more heat transfer from the target surface as compared to H/d=5 whereas H/d=7 gives 1 % increase in heat transfer as compared to H/d=9. Some of the curves overlap each other, this is due to interaction of jet.

The experimental regime is X/d = 0 (first copper plate) to X/d =109 (last copper plate). It is important to note that the drop in Nu is more pronounced at X/d=109. The main reason for this drop is that the copper plate 13 of the target surface is slightly bigger in size (to accommodate the length/width/clearance of the impingement channel) as compared to other plates, therefore the impinging jet does not hit at the geometric center of target copper plate # 13. In view of this eccentric impingement, the impinging hot air accumulates and tends to stagnate (leading to development of cross-flow). This stagnation accelerates build-up of cross flow and eventually decreases Nu.

Effect of Orifice-jet Plate Configuration on Local Nusselt Number

Figures 6-8 also demonstrate the variation of local Nu for the three orifice-jet configurations (centered, staggered, tangential) and H/d ratios as a function of non-dimensional location X/d on the target surface.

It can be observed that for a given situation (Re= 18800, outflow opposing the entry flow, for a given H/d), orifice-jet plate with centered holes gives better heat transfer characteristics as compared to staggered or tangential orifice-jet plate configurations. In general, peak value of local Nu has been observed in the range $20 \leq X/d \leq 50$ (the cross-flow is more dominant at other locations). The jet impingement is very effective in the range $20 \leq X/d \leq 50$. This can be attributed to strong impingement of air jets (with minimum crossflow) in the range $20 \leq X/d \leq 50$ as compared to exit locations. However, lower values of Nu are observed at X/d = 109 due to stagnation of hot air (as explained above, this reduces the heat transfer slightly at X/d = 109). It can be observed that some of the curves overlap each other at different points on the target plate. The overlapping of curves is due to interaction of jets.

For a given scenario with Re=18800 (outflow opposing the entry flow) and H/d=9, orifice jet plate with centered configuration gives about 17% higher Nu as compared staggered holes and staggered configuration gives about 3% higher Nu as compared to tangential holes. Also for the above situation (H/d=9, Re=18800 and Case-2) the peak value of local Nusselt number is 37.24 at X/d=49.2 for centered jets, Nu is 34.36 at X/d=32.4 for staggered jets, and Nu is 30.81 at X/d=32.4 for tangential jets.

Effect of Orifice-jet Plate Configuration on Averaged Nusselt Number

The average Nu is the average of Nu of all 13 copper plates on the target surface for a given situation (i.e. for a given Re, H/d, orifice-jet configuration, outflow orientation). In otherwords, the detailed results of a given scenario are averaged over the entire target plate to produce a single averaged Nu. To assess the effect of jet Reynolds number on average Nusselt number (Nu_{avg}), experimental runs were conducted for three different Reynolds numbers for a given feed channel width of H/d = 9. Figure 9 shows the effect of jet Re on average Nusselt number for a given H/d and for different orifice-jet configurations (for outflow opposing the entry flow). The Nu has been found to be sensitive to Re (Nu has been found to increase with increase in Re). The Nu_{avg} is highest for H/d=9 and for Re=18800 (i.e this scenario exhibits better heat transfer characteristics). The averaged Nusselt number increases correspondingly with an increase in the jet Re regardless of orifice-jet plate configuration and regardless of aspect ratio. This indicates that invariably Nusselt number is a strong function of Re. The higher values of average Nusselt number have resulted due to strong impingement of jets with minimum effect of cross-flow. Furthermore, the average Nu of plate-1 (centered holes) has been observed to be higher as compared to the Nu of other plate configuration (for a given Re, H/d, and outflow orientation opposing the inlet flow). For the above situation with Re=18800 and H/d=9, the percentage increase in average Nu has been found to be about 19% with centered holes as compared staggered orifice-jet plate. Also, the percentage increase in average Nu has been found to be about 4% with staggered jet-plate as compared to tangential orifice-jet plate configuration.

It is difficult to find out the exact experimental set-up in the literature similar to the one which has been developed in the present study for comparison of results, however, attempt has been made to make some comparison. Figure 10 compares the results of the present study with archival results of Huang et.al [22] for different jet Re and for different outflow orientations (for a given jet-orifice plate with centered jets). Huang's study focused on multiple array jets, however the present study concentrated on single array of centered/staggered/tangential jets (with an inclined target surface). Florschuetz [4] studied experimentally heat transfer distributions for jet array impingement. He considered circular jets of air impinging on heat transfer surface parallel to the jet orifice plate. The air after impingement was constrained in a single direction. Florschuetz presented Nu for centered and staggered hole patterns. The average Nusselt number is low in the present study. This may be because the present study involves single array of jets, whereas other studies considered multi array of jets.

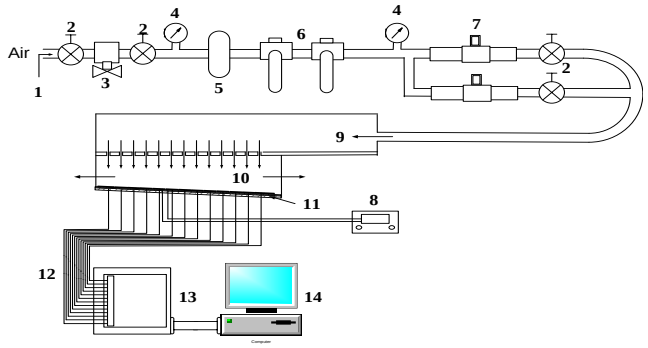

1- Compressed Air. 2- Valves.
3- Discharged Valve. 4- Pressure Gauges.
5- Settling Chamber. 6- Air and Oil Filters.
7- Digital Flow Meters. 8- Transformer.
9- Feeding Channel. 10- Impingement Channel.
11- Target Surface. 12- Thermocouples.
13- Data Acquisition. 14- Computer.

Figure 1: Schematic of the test section

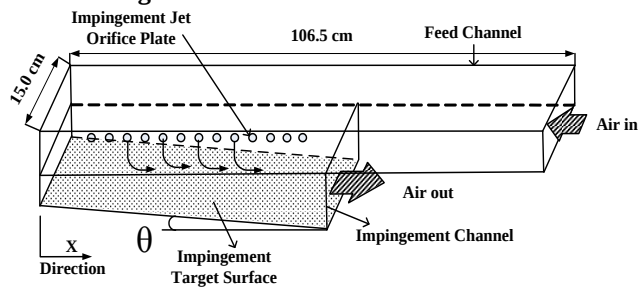

Figure 2.1: Three-dimensional view of the test section

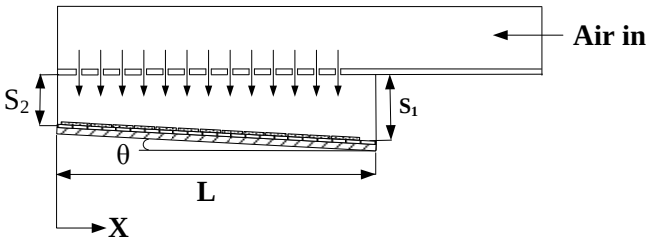

Figure 2.2: Inclination angle of the target surface

S_1= 3.5 cm, S_2= 2.0 cm, L=57.3 cm

$\theta = \tan^{-1}(57.3/1.5) = 1.5°$

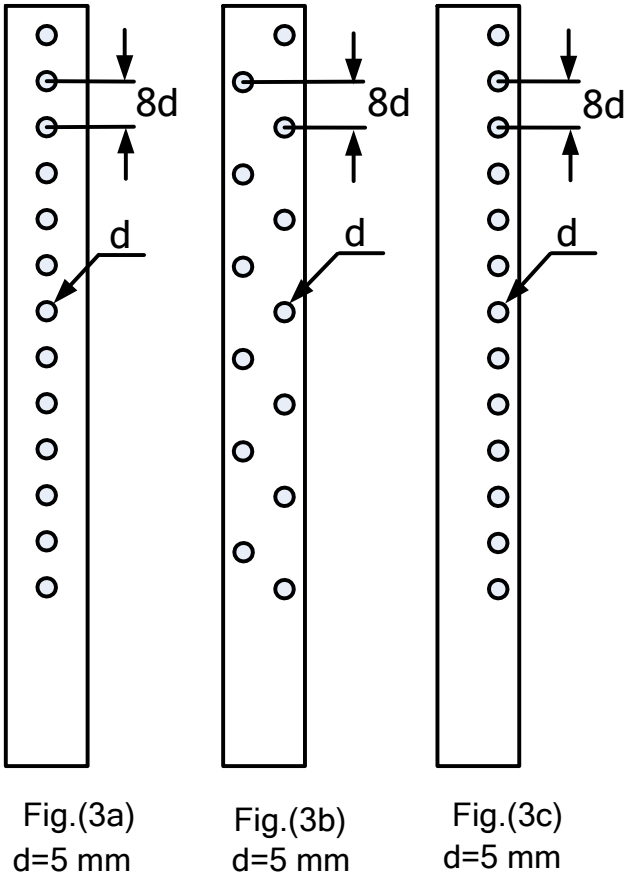

Figure 3: Illustration of three orifice-jet configurations with single array of jets (d = 5 mm) (Fig. 3a Centered holes, Fig. 3b Staggered holes, Fig. 3c Tangential holes)

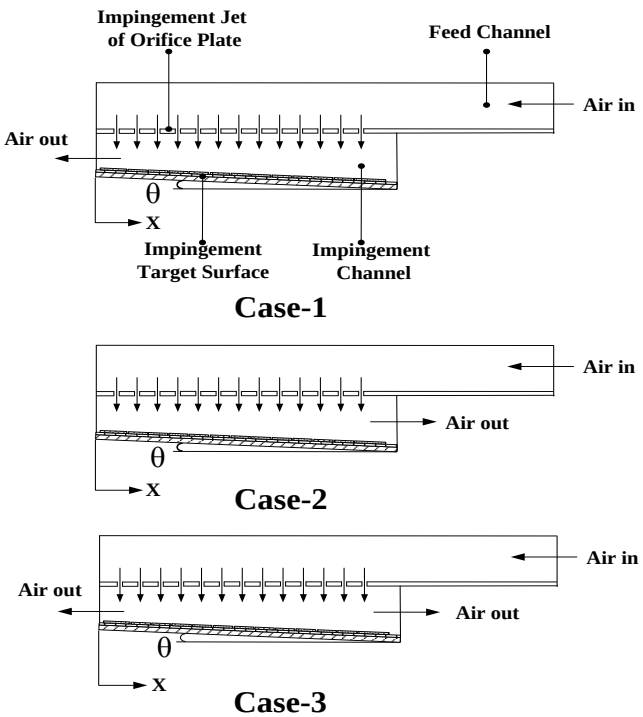

Figure 4: Illustration of three exit outflow orientations

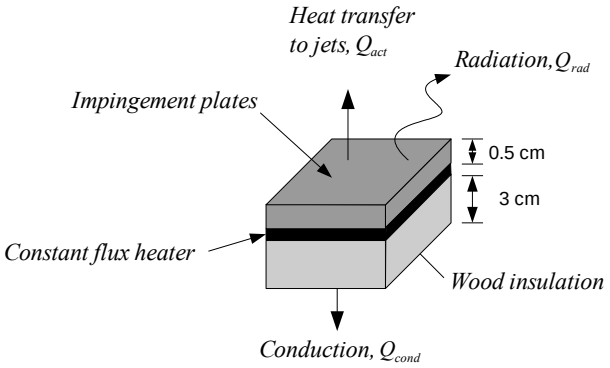

Figure 5: Overall energy balance over a small element of the impingement plate

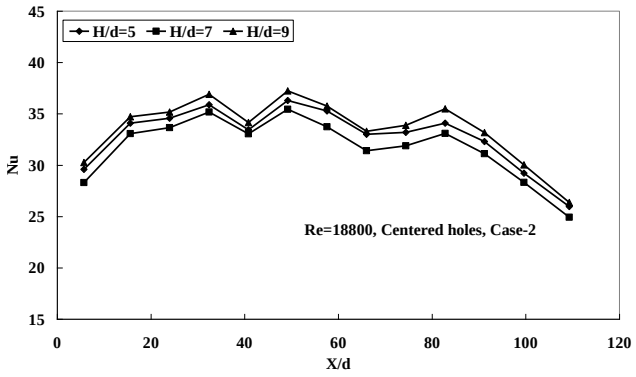

Figure 6: Nusselt number distribution for different aspect ratios and for outflow orientation opposing the entry flow (for jet-orifice plate with centered holes and for Re =18800)

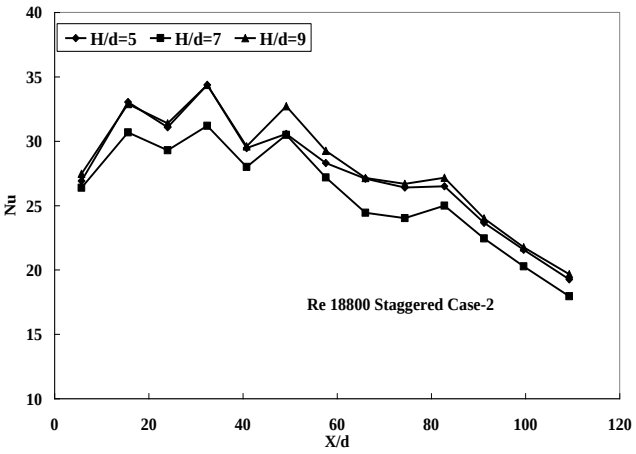

Figure 7: Nusselt number distribution for different aspect ratios and for outflow orientation opposing the entry flow (for jet-orifice plate with staggered holes and for Re =18800)

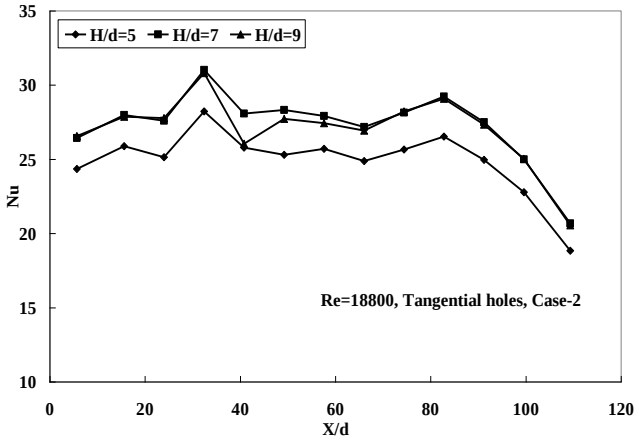

Figure 8: Nusselt number distribution for different aspect ratios and for outflow opposing the entry flow (for jet-orifice plate with tangential holes and for Re =18800)

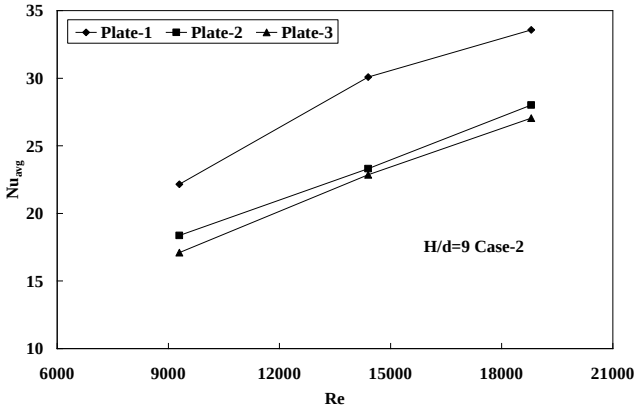

Figure 9: Average Nusselt number distribution for different jet Re and for different orifice jet-plate configurations (for aspect ratio H/d=9, for outflow orientation opposing the entry flow)

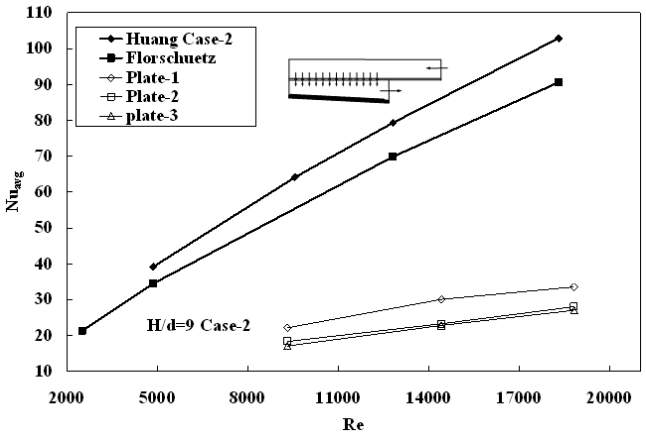

Figure 10: Comparison of Average Nusselt number of present study with archival studies for different jet Re and for different orifice-jet configurations (for H/d=9, for outflow opposing entry flow)

CONCLUSION REMARKS

The study has discussed in considerable depth the effect of orifice-jet plate configurations on feed channel aspect ratio (H/d) and on Nusselt number in a channel with inclined target surface cooled by single array of impinging jets (with outflow opposing the entry flow). In general, it has been observed that Nu is high for higher aspect ratios. For a given plate-1 with single array of equally spaced centered jets and for Re=18800 (outflow direction opposing with the entry flow), the local Nu for H/d=9 has been found to be greater than Nu of H/d=7 by 5%. Furthermore, Nu has been found to be relatively high in the mid-portion of the target surface while low at the ends of the target surface. This can be attributed to dominance of cross-flow at the exits. The average Nu of plate-1 (centered holes) has been observed to be higher as compared to the Nu of other plate configurations (for a given Re, H/d, and outflow orientation parallel to inlet flow). It has been noticed that plate-1 with centered orifice-jet configuration gives better heat transfer characteristics relatively as compared to other orifice-jet configurations. The percentage increase in average Nu has been found to be about 19% with centered holes as compared staggered orifice-jet plate. The percentage increase in average Nu has been found to be about 4% with staggered jet-plate as compared to tangential orifice-jet plate configuration. The averaged Nusselt number has been found to increase with in jet Re regardless of orifice-jet plate configuration The findings of the present experimental study and their availability in open literature offer valuable information for researchers and designers.

ACKNOWLEDGMENT

The present work was supported by Research Institute, King Fahd University of Petroleum and Minerals, Dhahran, Saudi Arabia. The authors would like to greatly appreciate the above support. without such support, this work would not have been possible.

NOMENCLATURE

$A_{cp,i}$	Area of each copper plate [m^2]
A_{total}	Area of all copper plate [m^2]
d	Diameter of the orifice jet [m]
h_i	Local convective heat transfer co-efficient [W/m^2K]
H	Width of the feed channel [m]
I	Current supplied to heater [Amp]
l	Length of the copper plate [m]
k_{air}	Thermal conductivity of air [W/m.K]
k_{wood}	Thermal conductivity of wood [W/m.K]
Nu_i	Local Nusselt number for each copper plate
Nu_{avg}	Average Nusselt number
q"	Heat flux from the heater [W/m^2]
$Q_{cp,i}$	Heat input for each copper plate [W]
Q_{actual}	Actual heat released from target surface [W]
$Q_{cond,i}$	Heat lost due to conduction [W]
$Q_{rad,i}$	Heat lost due to radiation [W]
Q_{total}	Total heat input [W]
Re	Jet Reynolds number
R	Resistance of the heater [ohm]
t	Thickness of wood block behind the heater [m]
T_{in}	Inlet temperature [^oC]
$T_{s,i}$	Surface temperature [^oC]
T_{surr}	Temperature of the surroundings [^oC]
T_w	Wood block temperature [^oC]
U	Uncertainty
V	Voltage supplied to the heater [V]
V_{avg}	Average velocity of all jets [m/s]
$\forall$	Volume flow rate [m^3/s]
X	Distance in the x-direction [m]
θ	Inclination Angle [1.5^o]

Subscripts

cp	Copper plate
i	Index number for each copper plate
j	Jet
w	Wood

Greek Symbols

ε	Emissivity
σ	Stefan-Boltzman constant [$W/(m^2K^4)$]
μ	Dynamic Viscosity [kg/(ms)]
ρ	Density [kg/m^3]

REFERENCES

[1] Chupp, P. R. E., Helms, H. E., McFadden, P. W. and Brown, T. R. (1969). Evaluation of internal heat-transfer coefficients for impingement-cooled turbine airfoils. *J. Aircraft*, 6, 203-208.

[2] Florschuetz, L. W., Metzger, D. E., Su, C. C., Isoda, Y. and Tseng, H. H. (1984). Heat transfer characteristics for jet array impingement with initial cross flow. *Journal of Heat Transfer*, 106 (1), 34-41.

[3] Metzger, D. E. and Bunker, R. S. (1990). Local heat transfer in internally cooled turbine airfoil leading edge regions: Part I – Impingement Cooling without Film Coolant Extraction. *Journal of Turbo machinery*, 112 (3), 451-458.

[4] Florschuetz, L. W., Metzger, D. E., Su, C. C., Isoda, Y. and Tseng, H. H. (1981). Stream-wise flow and heat transfer distributions for jet impingement with cross flow. *Journal of Heat Transfer*, 103 (2), 337-342.

[5] Dong, L. L., Leung, C. W. and Cheung, C. S. (2002). Heat transfer characteristics of premixed butane/air flame jet impinging on an inclined flat surface. *Heat and Mass Transfer*, 39 (1), pp. 19-26.

[6] Rasipuram, S. C. and Nasr, K. J. (2004). A numerically-based parametric study of heat transfer off an inclined surface subject to impinging air flow. *International Journal of Heat and Mass Transfer*, 47 (23), 4967-4977.

[7] Beitelmal, A. H., Saad, M. A. and Patel, C. D. (2000). Effect of inclination on the heat transfer

between a flat surface and an impinging two-dimensional air jet. *International Journal of Heat and Fluid Flow*, 21 (2), 156-163.

[8] Roy, S. and Patel, P. (2003). Study of heat transfer for a pair of rectangular jets impinging on an inclined surface. *International Journal of Heat and Mass Transfer*, vol. 46, no. 3, pp. 411-425.

[9] Ekkad, S. Huang, Yahoo. and Han, Je-Chin (2000). Impingement heat transfer measurements under an Array of Inclined Jets. *Journal of Thermophysics and Heat Transfer*, 14 (2), 286-288.

[10] Tawfek, A. A. (2002). Heat transfer studies of the oblique impingement of round jets upon a covered surface. *Heat and Mass Transfer*, 38 (6), 467-475.

[11] Seyedein, et. al. (1994). Laminar flow and heat transfer from multiple impinging slot jets with an inclined confinement surface. *International Journal of Heat and Mass Transfer,* 37 (13), 1867-1875.

[12] Yang, Y. and Shyu, C. H. (1998). Numerical study of multiple impinging slot jets with an inclined confinement surface. *Numerical Heat Transfer; Part A: Applications*, 33 (1), 23-37.

[13] Yan, X. and Saniei, N. (1997). Heat transfer from an obliquely impinging circular air jet to a flat plate. *International Journal of Heat and Fluid Flow*, 18 (6), 591-599.

[14] Hwang, J. J., Shih, N. C., Cheng, C, S., et. al. (2003). Jet-spacing effect on impinged heat transfer in a triangular duct with a tangential jet–array. *International Journal of Transfer Phenomena*, 5, 65-74.

[15] Ramirez, C., Murray, D. B., and Fitzpatrick, J. A. (2002). Convective heat transfer of an inclined rectangular plate. *Experimental Heat Transfer*, 15 (1), 1-18.

[16] Stevens, J. and Webb, B. W. (1991). Effect of inclination on local heat transfer under an axisymmetric free liquid Jet. *International Journal of Heat and Mass Transfer*, 34 (4-5), 1227-1236.

[17] Hwang, J. J. and Cheng, C. S.(2001). Impingement cooling in triangular ducts using an array of side-entry wall jets. *International Journal of Heat and Mass Transfer*, 44, 1053-1063.

[18] Hwang, J.J. and Cheng, T. T. (1999). Augmented heat transfer in a triangular duct by using multiple swirling jets. *Journal of Heat Transfer*, 121, 683-690.

[19] Hwang, J. J. and Chang, Y. (2000). Effect of outflow orientation on heat transfer and pressure drop in a triangular duct with an array of tangential jets. *Journal of Heat Transfer*, 122, 669-678.

[20] Hwang, J.J. and Cheng, C. S. (1999). Detailed heat transfer distributions in a triangular duct with an array of tangential jets. *Journal of Flow Visalizationa & Image Processing,* 6, 115-128.

[21] Taylor, B. N. and Kuyatt, C. E. (1994). Guidelines for evaluating and expressing the uncertainty of NIST measurement results. *National Institute of Standards and Technology*, 1297-1303.

[22] Hwang, Y., Ekkad, S. V. and Han, J. (1998). Detailed heat transfer distributions under an array of orthogonal impinging jets. *Journal of Thermophysics and Heat Transfer*, 12 (1), 73-79.